



Cite this: DOI: 10.1039/d4cc02594f

 Received 29th May 2024,  
Accepted 14th June 2024

DOI: 10.1039/d4cc02594f

rsc.li/chemcomm

## Mixing and matching *N,N*- and *N,O*-chelates in anionic Mg(I) compounds: synthesis and reactivity with $\text{RN}=\text{C}=\text{NR}$ and $\text{CO}^\dagger$

 Andrea O'Reilly,<sup>a</sup> Matthew D. Haynes,<sup>b</sup> Zoë R. Turner,<sup>b</sup>  
 Claire L. McMullin,<sup>\*c</sup> Sjoerd Harder,<sup>d</sup> Dermot O'Hare,<sup>\*b</sup>  
 J. Robin Fulton<sup>\*a</sup> and Martyn P. Coles<sup>\*a</sup>

Reduction of  $[\text{Mg}(\text{NON})_2]$  ( $[\text{NON}]^{2-} = [\text{O}(\text{SiMe}_2\text{NDipp})_2]^{2-}$ ,  $\text{Dipp} = 2,6\text{-iPr}_2\text{C}_6\text{H}_3$ ) affords Mg(I) species containing NON- and NNO-ligands ( $[\text{NNO}]^{2-} = [\text{N}(\text{Dipp})\text{SiMe}_2\text{N}(\text{Dipp})\text{SiMe}_2\text{O}]^{2-}$ ). The products of reactions with  $\text{iPrN}=\text{C}=\text{NiPr}$  and CO are consistent with the presence of reducing Mg(I) centres. Extraction with THF affords  $[\text{K}(\text{THF})_2]_2[\text{NNO}\text{Mg}-\text{Mg}\text{NNO}]$  with a structurally characterised Mg–Mg bond that was examined using density functional theory.

Since the initial report of  $(\text{BDI})\text{Mg}-\text{Mg}(\text{BDI})$  in 2007 (I, Fig. 1;  $\text{BDI} = [\text{HC}\{\text{C}(\text{Me})\text{NDipp}\}_2]^-$ ),<sup>1</sup> Mg(I) reagents have demonstrated their capacity to act as soluble, electron precise reducing agents.<sup>2</sup> The discovery of these compounds has undoubtedly fuelled the recent development and application of low valent group 2 (alkaline earth, Ae) metal complexes.<sup>3</sup> Indeed, over 35 examples of neutral Mg(I) species  $(\text{L})\text{Mg}-\text{Mg}(\text{L})$  ( $\text{L} = \text{monoanionic ligand}$ ) have now been structurally characterised. In contrast, examples in which the low valent magnesium centres are present in an anionic  $[(\text{L}')\text{Mg}-\text{Mg}(\text{L}')]^{2-}$  unit ( $\text{L}' = \text{dianionic ligand}$ ) are a recent addition to this important family of compounds (Fig. 1).

The first anionic Mg(I) compounds II were synthesised in a one-pot reaction of the neutral diimine or diamine with  $\text{MgCl}_2$  in the presence of excess potassium.<sup>4</sup> The products have a coplanar  $[(\text{L}')\text{Mg}-\text{Mg}(\text{L}')]^{2-}$  unit with THF-solvated potassium cations above and below the  $\text{MgN}_2\text{C}_2$  metallacycles. In 2021,

Hill and co-workers isolated the dimeric Na/Mg complex III by reducing the neutral diamido magnesium precursor with 5% Na/NaCl.<sup>5</sup> The structure showed non-solvated sodium cations with  $\text{Na} \cdots \pi(\text{arene})$  interactions to ligand substituents. The  $[(\text{L}')\text{Mg}-\text{Mg}(\text{L}')]^{2-}$  unit is twisted, with a long Mg–Mg bond. The most recent addition to this family IV, derives from the steric modulation of a rigid  $[\text{xanth-EtNON}^{\text{Ar}}]^{2-}$  backbone ( $[\text{xanth-EtNON}^{\text{Ar}}]^{2-} = 4,5\text{-Ar}_2\text{-2,7-Et}_2\text{-9,9-Me}_2\text{-xanthene}$ ). Previous work had shown that when  $\text{Ar} = 2,4,6\text{-Cy}_3\text{C}_6\text{H}_2$ , the dinitrogen complex  $[\text{K}\{\text{Mg}(\text{xanth-EtNON}^{\text{Ar}})\}]_2(\mu\text{-N}_2)$  was isolated,<sup>6</sup> presumed to be due to the ligand bulk preventing Mg–Mg bond formation and the resulting Mg(I) radicals reducing

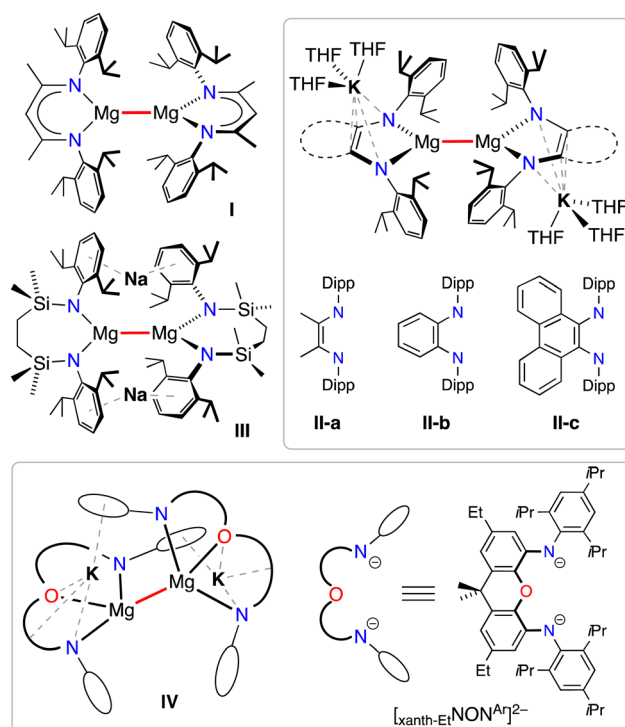


Fig. 1 Examples of neutral (I) and anionic (II, III and IV) Mg(I) compounds.

<sup>a</sup> School of Chemical and Physical Sciences, Victoria University of Wellington, PO Box 600, Wellington 6012, New Zealand. E-mail: martyn.coles@vuw.ac.nz, j.robin.fulton@vuw.ac.nz

<sup>b</sup> Chemistry Research Laboratory, Department of Chemistry, University of Oxford, Mansfield Road, Oxford OX1 3TA, UK. E-mail: dermot.ohare@chem.ox.ac.uk

<sup>c</sup> Department of Chemistry, University of Bath, Bath, BA2 7AY, UK. E-mail: cm2025@bath.ac.uk

<sup>d</sup> Inorganic and Organometallic Chemistry, Friedrich-Alexander-Universität, Erlangen-Nürnberg, Egerlandstraße 1, 91058 Erlangen, Germany

† Electronic supplementary information (ESI) available: Experimental details and characterization data; full details of computational experiments. CCDC 2357068 (1), 2357069 (2), 2357070 (3-Et<sub>2</sub>O) and 2357071 (4-THF). For ESI and crystallographic data in CIF or other electronic format see DOI: <https://doi.org/10.1039/d4cc02594f>

$N_2$ . Reducing the size of the Ar substituents to 2,4,6-*i*Pr<sub>3</sub>C<sub>6</sub>H<sub>2</sub> allowed Mg–Mg bond formation in **IV**.<sup>7</sup> The solid-state structure of **IV** adopts a folded structure with the potassium atoms coordinated *via*  $\eta^4$ -OCN<sub>2</sub> and  $\eta^6$ -aryl interactions to the ligands.

The reactivity of anionic Mg(i) compounds with a range of small molecules (H<sub>2</sub>, CO, N<sub>2</sub>O, THF),<sup>5,7,8</sup> and organic functional groups (alkynes, nitriles, carbodiimides, ketones, polyaromatic compounds)<sup>9</sup> has been explored, confirming the reductive capability of these species. We report herein the synthesis of a magnesium compound supported by the NON-ligand  $[(NON)]^{2-} = [O(SiMe_2NDipp)_2]^{2-}$ , its reduction to Mg(i) and the reactivity of the low-valent species with *i*PrN=C=NiPr and CO.

Prior to this work, Mg(NON)(THF)<sub>2</sub> was the only reported group 2 metal NON-compound, isolated as a product of over reduction and ligand transfer during the synthesis of a Bi(II) radical.<sup>10</sup> In this work the non-solvated compound was targeted as a precursor to reduced Mg(i) species, using an alkane elimination route between MgBu<sub>2</sub> and (NON)H<sub>2</sub> (Scheme 1). The reaction proceeded smoothly in hexane or toluene, affording colourless crystals of  $[Mg(NON)]_2$  (**1**).

Compound **1** is sparingly soluble in hydrocarbon solvents, preventing the acquisition of meaningful spectroscopic data at room temperature.<sup>11</sup> The crystal structure revealed a dimer located on an inversion centre (Scheme 1). The bidentate ligand adopts a  $\kappa N^1, O-\mu-N^2$ -coordination mode in which the oxygen atom is in a four-membered N–Si–O–Mg metallacycle and the pendant N2 atom bonds to the symmetry related Mg. We note that the Mg···Mg separation of 4.102(1) Å is too great to support a Mg–Mg bond in this dimeric arrangement, necessitating a reorganisation of the ligand to permit formation of the target  $[(L')Mg-Mg(L')]^{2-}$  unit.

The reduction of **1** by KC<sub>8</sub> in Et<sub>2</sub>O reproducibly forms a new product **A** (Scheme 2). <sup>1</sup>H NMR analysis indicated two distinct sets of ligand resonances in a 1 : 1 ratio that are consistent with a symmetric and a non-symmetric environment at magnesium. This is most clear from the three SiMe<sub>2</sub> singlets that appear at  $\delta_H$  0.38 (12H), 0.04 (6H) and –0.04 (6H). The symmetric environment at magnesium is consistent with a Mg(NON) group with a  $\kappa N, N'$ - or  $\kappa N, O, N'$ -coordination mode of the

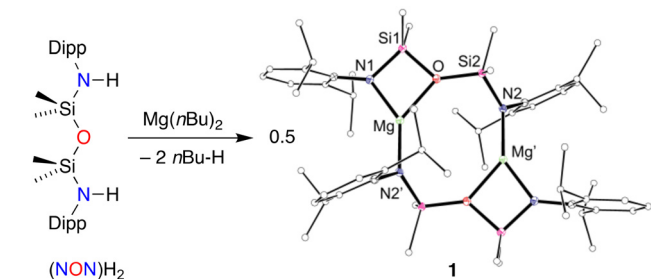
NON-ligand.<sup>10</sup> Based on NMR spectra of a related aluminium system, we attribute the non-symmetric ligand environment to a previously reported intramolecular 1,3-silyl retro-Brook rearrangement of the NON-ligand to form an *N,O*-chelated Mg(NNO) group  $[(NNO)]^{2-} = [N(Dipp)SiMe_2N(Dipp)SiMe_2O]^{2-}$ .<sup>12</sup> We are unable to crystallise **A** and cannot therefore assign it a precise chemical structure. Furthermore, analytical data does not allow us to discriminate between a discrete heteroleptic  $[(NON)Mg-Mg(NNO)]^{2-}$  unit or a mixture that also includes homoleptic  $[(NON)Mg-Mg(NON)]^{2-}$  and  $[(NNO)Mg-Mg(NNO)]^{2-}$  species. It is possible that a dynamic equilibrium exists, hindering crystallisation of a single species. However, onward reactivity confirms the presence of both  $K[Mg(NON)]$  and  $K[Mg(NNO)]$  groups in **A**.

Evidence for **A** reacting as a discrete heteroleptic  $[(NON)Mg-Mg(NNO)]^{2-}$  unit is inferred from its reaction with diisopropylcarbodiimide to form **2** (Scheme 2). Previous studies with **I** and **II-a** showed that addition of RN=C=NR (R = Cy, *t*Bu) afforded the magnesioamidinate species from the reductive insertion of carbodiimide into a Mg–Mg bond.<sup>1,9c</sup> The proposed mechanism involves initial *N*-coordination of the carbodiimide to one Mg centre, followed by migration of the second Mg to the sp<sup>2</sup> carbon of the carbodiimide.<sup>1,13</sup>

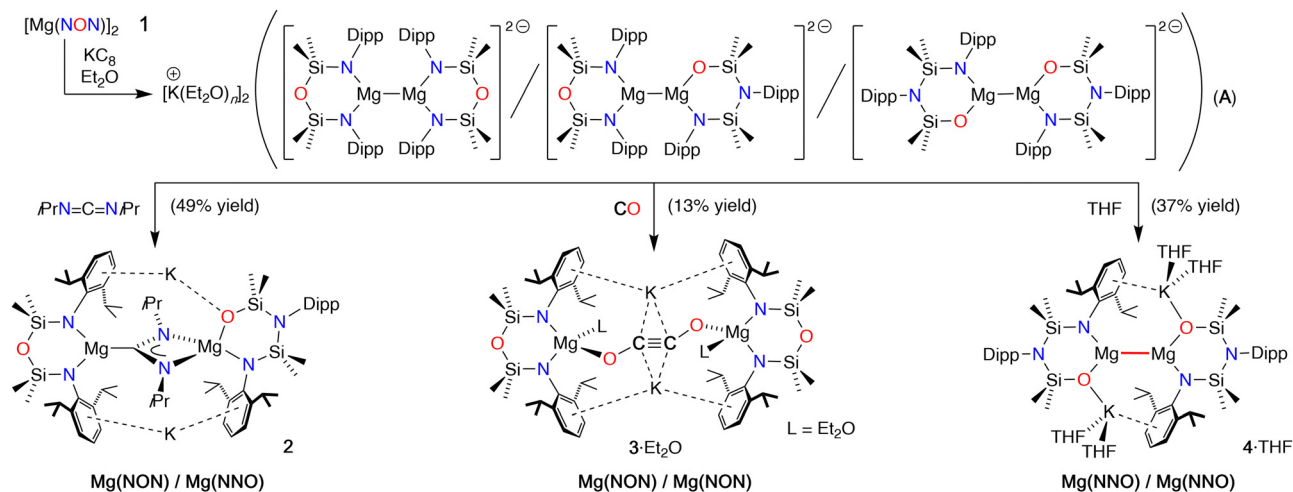
NMR spectra of **2** retain a 1 : 1 ratio of NON- and NNO-ligand resonances, with additional signals for magnetically equivalent NiPr groups, and a high frequency resonance at  $\delta_C$  226.1 for the CN<sub>2</sub> carbon atom. The crystal structure reveals both Mg(NON) and Mg(NNO) groups bridged by a  $[C(NiPr)_2]^{2-}$  unit (Fig. 2). The C–N distances in the amidinate unit (1.344(3)–1.358(3) Å) indicate delocalisation in the CN<sub>2</sub> fragment, confirming a two-electron reduction of the carbodiimide. The regiochemistry in **2** is consistent with *N*-coordination of the carbodiimide at the less sterically encumbered Mg(NNO) centre, followed by migration of the Mg(NON) fragment to the carbon atom.<sup>12a</sup>

Compounds **III**, **IV** and the aforementioned dimagnesium( $\mu$ -N<sub>2</sub>) complex reductively dimerise CO to afford ethynediolate complexes.<sup>5–7</sup> The reaction of **A** with 1 bar CO proceeded with an immediate colour change from yellow to red-orange, affording a low yield of crystals of **3**·Et<sub>2</sub>O (Scheme 2). The <sup>1</sup>H NMR spectrum showed only symmetric ligand environments, consistent with Mg(NON) fragments. The <sup>13</sup>C{<sup>1</sup>H} NMR spectrum showed a signal at  $\delta_C$  76.6, downfield of the  $[C_2O_2]^{2-}$  resonances noted in previous ethynediolate products ( $\delta_C$  50.2/55.3).

X-ray diffraction analysis of **3**·Et<sub>2</sub>O confirmed formation of the homoleptic ethynediolate complex, K<sub>2</sub>{[Mg(NON)(Et<sub>2</sub>O)]<sub>2</sub>( $\mu$ -C<sub>2</sub>O<sub>2</sub>)} containing Et<sub>2</sub>O solvated Mg(NON) groups (Fig. 3). Previous studies showing that the isomerisation of Al(NON) to Al(NNO) is exergonic<sup>12a</sup> suggest that the formation of Mg(NNO) groups during the synthesis of **A** is non-reversible. The absence of Mg(NNO) groups in **3**·Et<sub>2</sub>O therefore suggests that its formation involves the preferential reaction of CO with the Mg(NON) components of **A**, and may indicate the presence of symmetrical  $[(NON)Mg-Mg(NON)]^{2-}$  units. The structural parameters of the 'Mg(OC≡CO)Mg' unit closely resemble the previous examples,<sup>5,6,14</sup> with a short C–C bond of 1.211(8) Å and a slight *trans*-bent geometry (O2–C29–C29' = 164.6(6)°).



**Scheme 1** Synthesis and thermal displacement plot (30% probability; H-atoms omitted; peripheral carbons as spheres) of **1** (*r* = –*x*, 1 – *y*, –*z*). Selected bond lengths (Å) and angles (°): Mg–N1 1.9414(10), Mg–O 2.0605(9), Mg–N2' 1.9542(10), Mg···Mg' 4.102(1); N1–Mg–O 77.54(4), N1–Mg–N2' 143.74(5), O–Mg–N2' 138.48(4).



Scheme 2 Formation of **A** and reaction with  $\text{iPrN}=\text{C}=\text{NiPr}$ , CO and THF to afford **2**, **3**· $\text{Et}_2\text{O}$  and **4**·THF (isolated yields reported).

Extraction of **A** with THF afforded a mixture of products including  $\text{K}_2[\text{NON}]$ , and the new compound **4**·THF that was isolated by fractional crystallisation in 37% yield. The  $^1\text{H}$  NMR spectrum of **4**·THF shows splitting according to a compound containing only NNO-ligands. This is confirmed by X-ray diffraction, revealing **4**·THF as the anionic  $\text{Mg}(\text{i})$  species,  $[(\text{NNO})\text{Mg}-\text{Mg}(\text{NNO})]^{2-}$  charge balanced with two  $[\text{K}(\text{THF})_2]^+$  cations (Fig. 4). This result indicates either an analogous redistribution of the  $[\text{Mg}(\text{L}')^-]$  fragments from a mixture present in **A**, or isomerisation of the  $\text{Mg}(\text{NON})$  group to the more stable  $\text{Mg}(\text{NNO})$  isomer during the extraction with THF. There is no residual electron density in the region expected for hydride ligands, confirming formation of the anionic  $\text{Mg}(\text{i})$  compound (Fig. S24, ESI $^\dagger$ ). The Mg–Mg bond length (2.9393(11) Å) is in the range reported for (solvent free)

(L)Mg–Mg(L) compounds (2.7907(9)–3.0513(8) Å),<sup>15</sup> and is shorter than found in the anionic  $\text{Mg}(\text{i})$  complexes **II** (3.2077(10) Å/3.2124(11) Å)<sup>5</sup> and **III** (3.1369(15) Å).<sup>14</sup> We attribute the short bond to the reduction in steric stress imparted by the NNO-isomer, and the reduction in electron density at Mg that results from the high electronegativity of the O-ligand.

DFT analysis of **I** and **IV** revealed a non-nuclear attractor (NNA) at the centre point of the Mg–Mg bond.<sup>7,16</sup> This feature was not prominent in the core of **III**,<sup>5</sup> which the authors suggest is best described as a  $[\text{Mg}_2\text{Na}_2]^{4+}$  unit. Investigation of **4**·THF by DFT (see ESI $^\dagger$  for details) show that the HOMO corresponds to the Mg–Mg  $\sigma$ -bond with equal contribution from both metals and a high  $s$ -character of  $\sim 93\%$  (Fig. 5a). Natural bond order (NBO) calculations show a Mg–Mg Wiberg bond index (WBI) of 0.724, with NPA charges  $q_{\text{Mg}} = +1.00$  and  $q_{\text{K}} = +0.88$ . These values compare well with those reported for **III** (WBI = 0.656,  $q_{\text{Mg}} = +1.03$  and  $q_{\text{Na}} = +0.84$ ),<sup>5</sup> and **IV** (WBI = 0.694,  $q_{\text{Mg}} = +0.97$

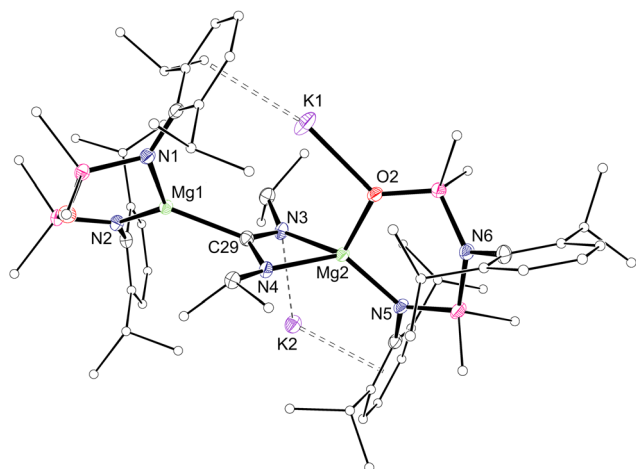


Fig. 2 Thermal displacement plot (30% probability; H-atoms omitted; peripheral carbons as spheres) of one of the independent molecules of **2**. Selected bond lengths (Å) and angles ( $^\circ$ ): Mg1–N1 2.0594(19), Mg1–N2 2.0415(19), Mg2–N5 2.0513(19), Mg2–O2 1.9122(16), C29–N3 1.358(3), C29–N4 1.344(3), Mg1–C29 2.232(2), Mg2–N3 2.1737(19), Mg2–N4 2.069(2); N1–Mg1–N2 123.18(8), N5–Mg2–O2 106.09(8), N3–Mg2–N4 63.51(7).

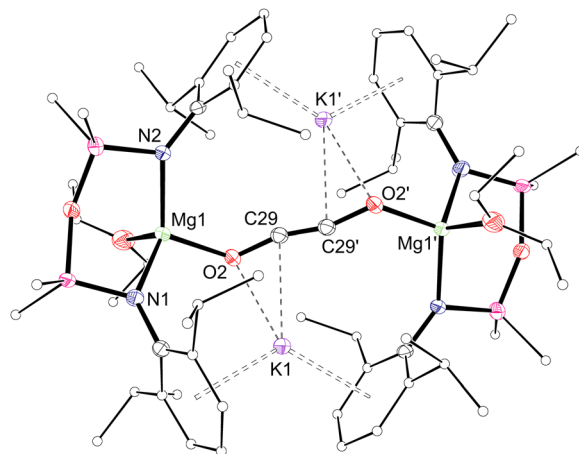


Fig. 3 Thermal displacement plot (30% probability; H-atoms omitted; peripheral carbons as spheres) of one of the independent molecules of **3**· $\text{Et}_2\text{O}$ . Selected bond lengths (Å) and angles ( $^\circ$ ): Mg1–N1 2.044(4), Mg1–N2 2.049(3), Mg1–O2 1.936(3), O2–C29 1.309(5), C29–C29' 1.211(8); N1–Mg1–N2 121.24(17), O2–C29–C29' 164.6(6).

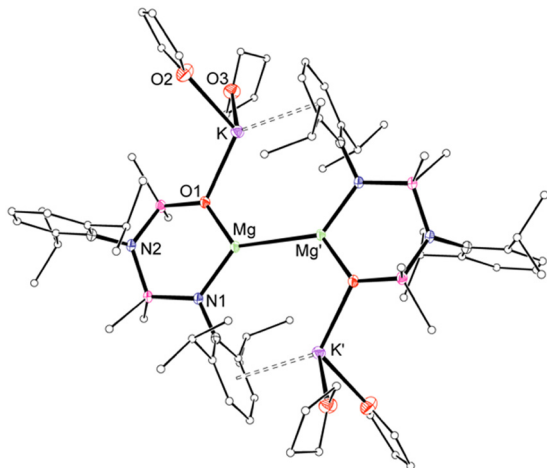


Fig. 4 Thermal displacement plot (30% probability; H-atoms omitted; peripheral carbons as spheres) of **4-THF** ( $\ell' = -x, -y, 2 - z$ ). Selected bond lengths (Å) and angles ( $^\circ$ ): Mg–Mg' 2.9393(11), Mg–N1 2.0493(15), Mg–O1 1.9203(13), O1–K 2.5859(13); N1–Mg–O1 106.37(6), N1–Mg–Mg' 131.70(5), O1–Mg–Mg' 121.91(5), Mg–O1–K 109.97(6).

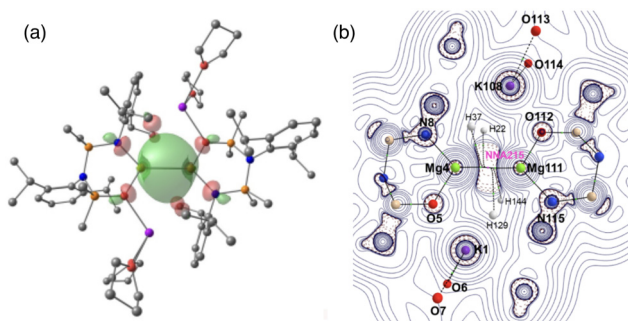


Fig. 5 (a) HOMO of **4-THF**. (b) Laplacian distribution for **4-THF**, showing non-nuclear attractor (NNA215) at the centre of the Mg–Mg bond. Both calculated at the BP86/6-311++G\*\*//BP86/BS1 level of theory.

and  $q_K = +0.90$ ).<sup>6</sup> An NNA of 0.72 electrons is present in the middle of the Mg–Mg bond in **4-THF** (Fig. 5b), similar to that noted in **I** (0.8 electrons).<sup>16</sup>

In conclusion, we have demonstrated that the reduction of the  $[\text{Mg}(\text{NON})]_2$  dimer **1** affords product **A**, formulated as containing  $\text{K}[\text{Mg}(\text{NON})]$  and  $\text{K}[\text{Mg}(\text{NNO})]$  units. Although the composition of **A** has not been explicitly identified and an equilibrium of different species may be present, analytical data and reactivity studies confirm the presence of reducing  $\text{Mg}(\text{NON})$  and  $\text{Mg}(\text{NNO})$  groups. Isolation and structural characterisation of  $[\text{K}(\text{THF})_2]_2[(\text{NNO})\text{Mg}-\text{Mg}(\text{NNO})]$  (**4-THF**) prompted analysis by DFT, showing a non-nuclear attractor of 0.72 electrons at the centre of the Mg–Mg bond. Access to both  $\text{K}[\text{Mg}(\text{NON})]$  and  $\text{K}[\text{Mg}(\text{NNO})]$  groups from **A** may expand the scope of reactivity compared with a system in which only one ligand-type was available. This flexibility imparted by the opportunity to 'mix and match'  $[\text{Mg}(\text{L}')]^-$  fragments according to the reaction may be important in stabilising the reduction products and will form part of our ongoing investigations.

A. O'. R., M. P. C. and J. R. F. acknowledge funding from the Royal Society Te Apārangi (MFP-VUW2020). M. D. H. acknowledges funding from the EPSRC Centre for Doctoral Training in Inorganic Chemistry for Future Manufacturing (OxICFM), EP/S023828/1, and the RSC for a Researcher Development and Travel Grant. C. L. M. acknowledges the RSC Research Enablement Grant (E21-8355738114). The authors gratefully acknowledge the University of Bath's Research Computing Group (<https://doi.org/10.15125/b6cd-s854>) for their support in this work.

## Data availability

The data supporting this article have been included as part of the ESI†

## Conflicts of interest

There are no conflicts to declare.

## Notes and references

- 1 S. P. Green, C. Jones and A. Stasch, *Science*, 2007, **318**, 1754–1757.
- 2 (a) C. Jones, *Nat. Rev. Chem.*, 2017, **1**, 0059; (b) A. Stasch and C. Jones, *Dalton Trans.*, 2011, **40**, 5659–5672.
- 3 (a) J. T. Boronski, *Dalton Trans.*, 2024, **53**, 33–39; (b) L. A. Freeman, J. E. Walley and R. J. Gilliard, *Nat. Synth.*, 2022, **1**, 439–448; (c) K. M. Fromm, *Coord. Chem. Rev.*, 2020, **408**, 213193.
- 4 (a) Y. Liu, S. Li, X.-J. Yang, P. Yang and B. Wu, *J. Am. Chem. Soc.*, 2009, **131**, 4210–4211; (b) M. Ma, H. Wang, J. Wang, L. Shen, Y. Zhao, W.-H. Xu, B. Wu and X.-J. Yang, *Dalton Trans.*, 2019, **48**, 2295–2299.
- 5 H.-Y. Liu, R. J. Schwamm, S. E. Neale, M. S. Hill, C. L. McMullin and M. F. Mahon, *J. Am. Chem. Soc.*, 2021, **143**, 17851–17856.
- 6 R. Mondal, M. J. Evans, T. Rajeshkumar, L. Maron and C. Jones, *Angew. Chem., Int. Ed.*, 2023, **62**, e202308347.
- 7 R. Mondal, M. J. Evans, D. T. Nguyen, T. Rajeshkumar, L. Maron and C. Jones, *Chem. Commun.*, 2024, **60**, 1016–1019.
- 8 (a) H.-Y. Liu, S. E. Neale, M. S. Hill, M. F. Mahon, C. L. McMullin and B. L. Morrison, *Chem. Commun.*, 2023, **59**, 3846–3849; (b) H.-Y. Liu, S. E. Neale, M. S. Hill, M. F. Mahon, C. L. McMullin and E. Richards, *Angew. Chem., Int. Ed.*, 2023, **62**, e202213670.
- 9 (a) L. Yang, Y. Zhang, Y. Zhao and X.-J. Yang, *Polyhedron*, 2023, **244**, 116632; (b) J. Wang, J. Wang, L. Shen, Y. Zhao, B. Wu and X.-J. Yang, *Organometallics*, 2019, **38**, 2674–2682; (c) L. Yang, Y. Qu, J. Wang, W. Xu, Y. Zhao and X.-J. Yang, *Chem. – Eur. J.*, 2023, **29**, e202301266; (d) H.-Y. Liu, S. E. Neale, M. S. Hill, M. F. Mahon, C. L. McMullin and E. Richards, *Organometallics*, 2024, **43**, 879–888.
- 10 R. J. Schwamm, J. R. Harmer, M. Lein, C. M. Fitchett, S. Granville and M. P. Coles, *Angew. Chem., Int. Ed.*, 2015, **54**, 10630–10633.
- 11  $^1\text{H}$  and  $^{13}\text{C}\{^1\text{H}\}$  NMR spectra recorded at 373 K show a symmetric ligand environment (Fig. S3 and S4, ESI†). The addition of THF to aid solubilisation forms a partially solvated dimer. Further details and related studies with heavier group 2 NON-compounds will be the subject of a forthcoming publication.
- 12 (a) A. O'Reilly, M. G. Gardiner, C. L. McMullin, J. R. Fulton and M. P. Coles, *Chem. Commun.*, 2024, **60**, 881–884; (b) F. Haftbaradaran, G. Mund, R. J. Batchelor, J. F. Britten and D. B. Leznoff, *Dalton Trans.*, 2005, 2343–2345; (c) F. Haftbaradaran, A. M. Kuchison, M. J. Katz, G. Schatte and D. B. Leznoff, *Inorg. Chem.*, 2008, **47**, 812–822.
- 13 L. Xiao, W. Chen, L. Shen, L. Liu, Y. Xue, Y. Zhao and X.-J. Yang, *Chem. Commun.*, 2020, **56**, 6352–6355.
- 14 R. Mondal, K. Yuvaraj, T. Rajeshkumar, L. Maron and C. Jones, *Chem. Commun.*, 2022, **58**, 12665–12668.
- 15 (a) X. Cao, J. Li, A. Zhu, F. Su, W. Yao, F. Xue and M. Ma, *Org. Chem. Front.*, 2020, **7**, 3625–3632; (b) T. X. Gentner, B. Rösch, G. Ballmann, J. Langer, H. Elsen and S. Harder, *Angew. Chem., Int. Ed.*, 2019, **58**, 607–611.
- 16 J. A. Platts, J. Overgaard, C. Jones, B. B. Iversen and A. Stasch, *J. Phys. Chem. A*, 2011, **115**, 194–200.